# Drawing behaviour, mechanical properties and structure of poly(*p*-phenylene sulphide) fibres

**P. L. Carr and I. M. Ward**
*Department of Physics, University of Leeds, Leeds LS2 9JT, UK*
*(Received 30 March 1987; accepted 15 May 1987)*

Poly(*p*-phenylene sulphide), (PPS), in the form of a multifilament spun yarn, was drawn over a heated roller (the pin) to a range of draw ratios from 1.26 to 4.8 at various pin temperatures from 70°C to 100°C. Annealed samples were also prepared using a second high temperature annealing zone in the drawing process, using a heated plate at temperatures between 150°C and 220°C. The maximum birefringence achieved was 0.270 compared with a theoretical maximum of 0.330 calculated from bond polarizabilities and bond angles suggesting that the drawing process conditions were close to optimization. From birefringence, shrinkage, and shrinkage force measurements average molecular network parameters were derived and in the light of these parameters the mechanical properties of oriented PPS fibres are compared with the mechanical properties of poly(ethylene terephthalate), (PET), and poly(ethylene methylterephthalate), (PEMT), fibres. The network parameters suggest that the PPS network has a higher density of entanglements than PET, connected by stiffer chains with fewer random links. However, recent measurements of the crystal modulus of PPS suggest that the planar zig-zag conformation of the molecule is responsible for the lower modulus of 8 GPa for PPS yarns compared with 16 GPa achieved with PET, rather than failure to achieve a sufficiently high molecular orientation.

**(Keywords: poly(phenylene sulphide); mechanical properties; fibre; birefringence; molecular conformation; crystal modulus)**

## INTRODUCTION

The good thermal and chemical stability of poly(*p*-phenylene sulphide), (PPS), has led to the commercial development of this polymer for certain specialized outlets, but the mechanical properties of the oriented material so far reported have not been such that it can be considered as a replacement for other materials such as polyamide and polyester in outlets where strength and toughness are at a premium. Ito and Porter[1] report an initial modulus of 5 GPa and tensile strength of 0.13 GPa at a draw ratio of approximately 3.5 using a solid state co-extrusion process and commercially drawn fibre has typically an initial modulus of 5–6 GPa and a tensile strength of 0.5 GPa. These properties are rather lower than those achieved with polyamide and polyester fibres drawn to high draw ratios for industrial end uses.

The objective of this investigation was to determine whether higher draw ratios and higher molecular orientations could be achieved in PPS fibres, leading to enhanced mechanical properties, or indeed whether the molecular orientation already obtained by previous workers was close to the practical and theoretical limit and the properties were therefore limited by the properties of the molecule and network structure. Experimental measurement and theoretical calculation of the longitudinal crystal modulus was also undertaken in this laboratory[2] so that further comparison with drawn fibre properties could be made.

The concept of a molecular network and its role in controlling and limiting the molecular orientation imposed by cold drawing poly(ethylene terephthalate), (PET), has been discussed in several previous publications[3,4] and a similar procedure has been followed here to derive network parameters from birefringence and shrinkage force measurements using the equations of rubber elasticity theory. The theoretical maximum birefringence for perfectly aligned molecular chains was also derived from calculated and published values of bond polarizabilities, so that the efficiency of the optimized drawing process could be assessed and compared with the drawing of other polymers, and so that the mechanical properties could also be compared with those of other polymers relative to the degree of molecular orientation achieved.

Spun yarns with low pre-orientation (and of total decitex 990, comprising 30 filaments) were kindly supplied by The Phillips Petroleum Company, Bartlesville, Oklahoma, USA.

## EXPERIMENTAL

### *Drawing and annealing*

The spun yarn samples were drawn to various draw ratios using one turn on a 7.5 cm diameter heated roller (the pin) to localize the draw point and initiate drawing between two cold rollers rotating at different speeds. Drawing temperatures quoted are pin surface temperatures at the point at which the yarn leaves the pin. Achieved draw ratios $\lambda_a$ are quoted, based on yarn decitex measurements.

Annealed samples were obtained by placing a 45 cm heated plate between the heated pin and the final draw roll. Temperatures quoted are mid point surface temperatures.

0032-3861/87/122070-07$03.00

In the combined drawing and annealing process (the pin and plate process), the draw ratio divides between the primary draw at the draw temperature on the hot pin and the secondary draw or hot stretch on the hot plate. The primary draw is usually the larger, but the division between the two is complex and varies with temperature and draw ratio and the polymer used. This has not been investigated in the present study. However, some yarns were annealed in a separate hot stretching process in which case the two component draw ratios are defined.

A low draw speed of 10 m/min was used throughout these experiments, therefore to some extent the properties obtained can be regarded as an upper limit. However a deterioration in drawn yarn quality with draw speed might be remedied by more sophisticated equipment and increased temperatures.

*Tensile testing*

The initial modulus, failure stress and failure strain were measured at room temperature, 20°C, using an Instron tensile testing machine with a sample length of 10 cm and a rate of extension of 50% per min. To give clean breaks and reduce the effect of filament variability 2–3 turns per inch twist was inserted in the yarn samples.

*Birefringence measurements*

Birefringence measurements were made in order to compare the molecular orientation achieved with the theoretical maximum orientation calculated from the optical anisotropy of the aligned monomer unit. Optical retardation was measured using an Ehringhaus compensator with a Zeiss polarizing microscope. Poly(*p*-phenylene sulphide) has a high birefringence and dispersion and the zero order black fringe in white light fringes undergoes six fringe 'jumps'[5], at the highest birefringence measured. This necessitated a calibration procedure using a filament wedge to determine corrections from the observed blue/black fringe to the correct zero order fringe. To ensure that this calibration procedure was correct, several filaments were checked using an Interference microscope and Cargill birefringent liquids. This very accurate method agreed well with the quick polarizing microscope method.

*Shrinkage force measurements*

Shrinkage force measurements were made in order to determine the characteristics of the PPS molecular network which controls the response of the material to applied stress. These measurements were made in silicone oil at 100°C using a special apparatus described by Capaccio and Ward[6]. In these measurements it was assumed that in the short time taken by the specimen to heat up and undergo thermal expansion, the shrinkage force did not decay significantly. This consideration is discussed by O'Neill[7].

*Shrinkage*

Finally, free shrinkage measurements were also made at 100°C in silicone oil. The correspondence between draw ratio and subsequent shrinkage has a bearing on the validity of the shrinkage force measurements and the shrinkage measurements can also be used to obtain a value of the number of monomer units per statistical chain length between entanglements.

## RESULTS

*Drawing behaviour*

Satisfactory drawing performance was obtained at pin surface temperatures between 80°C and 100°C. Below 80°C longitudinal voids formed, particularly at the centre of the filaments, extending throughout the whole filament cross section as the draw ratio was increased. Above 100°C drawing was not possible due to yarn sticking to the pin surface and due to filaments failing in a ductile manner.

*Figure 1* shows that in terms of failure stress, an optimum drawing temperature exists close to the $T_g$ of the material 85°C.[1]

Draw ratios between 1.26 and 5.0 were used. At a draw temperature of 80°C the maximum achieved draw ratio $\lambda_a$, was 4.4 and at 90°C the maximum achieved draw ratio was 4.8.

*Annealing*

*Figure 2* shows that an increase in annealing temperature from 140°C to 220°C gave a small increase in failure stress but no significant increase in initial modulus. The addition of a higher temperature annealing zone in the drawing process did not allow a significantly higher draw ratio to be achieved.

*Mechanical properties*

Failure stress and initial modulus have been calculated from the load/extension curves using a density of

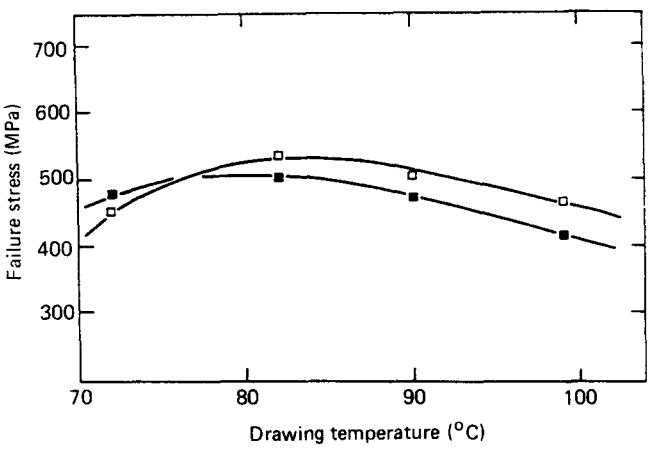


**Figure 1** Failure stress vs. drawing temperature for pin drawn yarn. □, actual draw ratio $\lambda_a = 3.7$; ■, $\lambda_a = 4.1$

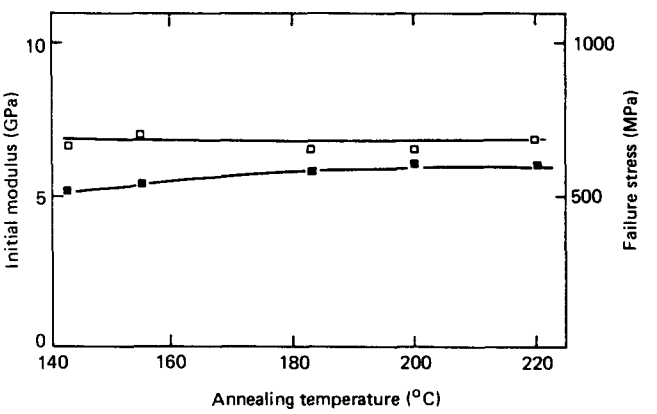


**Figure 2** Failure stress and initial modulus vs. annealing temperature at a draw temperature of 85°C and draw ratio $\lambda_a = 4.1$. □, initial modulus; ■, failure stress

1.32 g cm$^{-3}$ for oriented amorphous yarns and 1.35 g cm$^{-3}$ for oriented crystalline yarns. These values were obtained from measurements on drawn and annealed samples using a density gradient column containing a solution of potassium iodide.

*Figure 3* shows initial modulus as a function of draw ratio. At 90°C the initial modulus is similar to that of PET drawn to the same temperature[8]. However, a reduction in draw temperature is less effective in increasing the modulus than for PET and, when drawn at 80°C, the modulus of PPS is significantly lower than that of PET. There is a small increase in modulus of 8% when an annealing zone is included in the drawing process.

A maximum initial modulus of 8 GPa was achieved compared with values obtained for high tenacity PET of approximately 16 GPa.

*Figure 4* shows the failure stress plotted as a function of draw ratio. Here the effect of draw temperature is small in the range 80°C–90°C and the significant effect at high draw ratios is now that of an annealing stage which gives at best a 30% increase in failure stress.

*Figure 5* shows the failure stress as a function of failure strain for draw temperatures of 80°C and 90°C. Yarns drawn to low draw ratios at higher draw temperatures tend to have a higher failure stress at a given strain. However, after a second draw this failure stress is not increased proportionally and the maximum failure stress lies on the curve shown. A very uniform spun yarn might be drawn to an extensibility of 10% or less, therefore giving a failure stress of approximately 800 MPa compared with 1000–1100 MPa for PET drawn to the same extensibility.

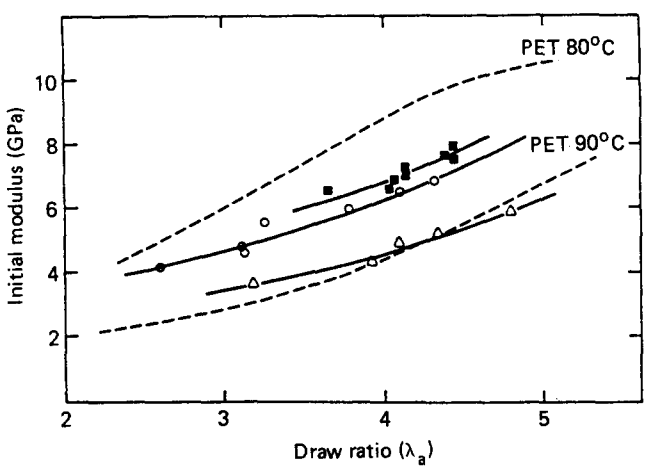


**Figure 3** Initial modulus vs. draw ratio. ○, pin only at 80°C; △, pin only at 90°C; ■, pin 90°C, plate 180°C

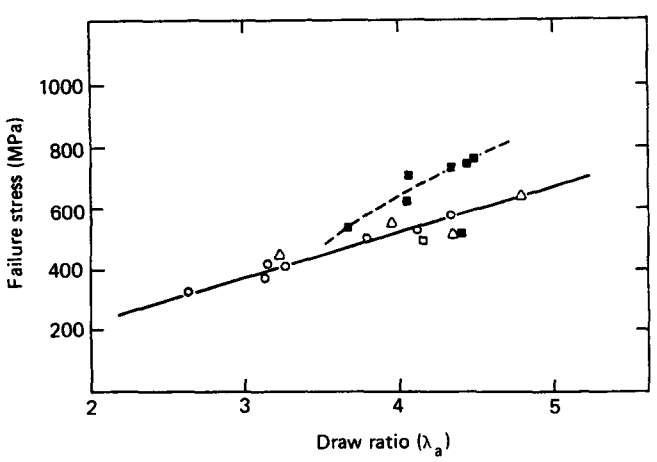


**Figure 4** Failure stress vs. draw ratio. Key as *Figure 3*

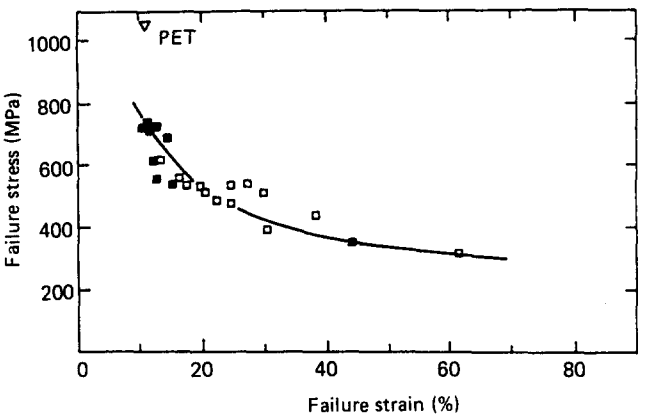


**Figure 5** Failure stress vs. failure strain. □, pin only; ■, pin and plate drawing

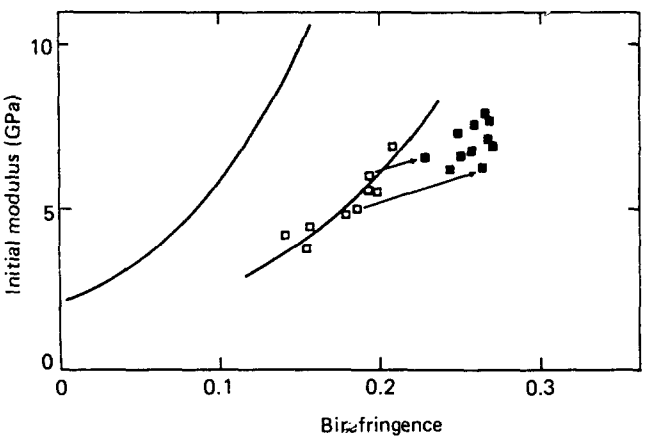


**Figure 6** Initial modulus vs. birefringence. Key as *Figure 5*

*Figure 6* shows the initial modulus of drawn PPS yarns plotted as a function of birefringence and is compared with data for PET obtained by Brody[9]. It can be seen that the initial modulus of PET rises more steeply as it approaches its maximum birefringence, (which is in practical yarn processes approximately 0.190) than does the modulus of PPS.

PET can be drawn to a birefringence close to its maximum in a single stage drawing process at a draw temperature just above $T_g$. In contrast, the maximum birefringence obtained in the single stage process with PPS was 0.208, and annealing resulted in an increase in birefringence to give values approaching 0.270. Two samples are indicated which derive from annealing yarn at constant length after a preliminary drawing process, and the parent yarns are indicated. It is interesting to note that the larger increase in birefringence is obtained from the yarn drawn to a rather lower initial draw ratio and birefringence. As indicated previously, annealing and crystallization produces only a modest increase in initial modulus.

The more important mechanical properties are listed in *Table 1* including birefringence measurements.

## SHRINKAGE, SHRINKAGE FORCE AND YARN STRUCTURE

### *Shrinkage measurements*

If all the draw ratio applied to the polymer network is

recovered during shrinkage then the shrinkage and draw ratio are related by the equation

$$\lambda_T = \frac{1}{1-S}$$

where $\lambda_T$ is the total network draw ratio including the contribution from spinning, i.e. $\lambda_T = \lambda_a \lambda_s$, $\lambda_a$ is the achieved draw ratio, $\lambda_s$ is equivalent extension of the network which occurs during spinning and $S$ is the fractional shrinkage. The shrinkage of the drawn yarn was measured in silicone oil at 100°C. The results are given in *Table 2* and shown in *Figure 7* where $1/1-S$ is plotted against the applied draw ratio $\lambda_a$. From the initial slope of this graph, $\lambda_s$, was found to be 1.07. *Figure 7* also shows that the network extension is totally recovered during shrinkage until the yarn is drawn to draw ratios greater than 2.6 when from *Table 2* the birefringence is seen to be $141 \times 10^{-3}$. X-ray diffraction photographs and density measurements have shown that crystallization begins to be significant at this orientation and therefore stress induced crystallization is responsible for the sharp reduction in shrinkage shown in *Figure 7* at a draw ratio of approximately 3.

From simple rubber elasticity theory[10] the birefringence is related to the total network extension $\lambda_T$ by the equation:

$$\Delta n = \frac{2\pi}{45} \frac{(\bar{n}^2+2)^2}{\bar{n}} N_0(\alpha_1 - \alpha_2)(\lambda_T^2 - \lambda_T^{-1}) \quad (1)$$

where $\bar{n}$ is the mean refractive index of the fibre, $N_0$ is the number of chain segments between entanglements per unit volume, $(\alpha_1 - \alpha_2)$ is the optical anisotropy of a statistical random link in these chain segments.

In *Figure 8* the birefringence is plotted against a function of the total network extension ratio $\lambda_T$, where $\lambda_T$ includes the actual draw ratio $\lambda_a$ and the correction obtained from *Figure 7* for the equivalent extension ratio of the spun yarn. The correction appears to be reasonable

**Table 1** Mechanical properties and birefringence of drawn yarns

| Sample number | Draw temperature (°C) | Plate temperature (°C) | Nominal draw ratio $\lambda_a$ | Failure stress (MPa) | Failure strain (%) | Initial modulus (GPa) | Birefringence $\times 10^{-3}$ |
|---|---|---|---|---|---|---|---|
| PPS 1 | 80 | – | 3.1 | 355 | 44.2 | 4.8 | 179.2 |
| 2 | 80 | – | 3.24 | 393 | 30.6 | 5.57 | 193.8 |
| 3 | 80 | – | 3.77 | 486 | 22.5 | 5.98 | 194.5 |
| 4 | 80 | – | 4.32 | 556 | 16.5 | 6.89 | 208.7 |
| 6 | 80 | – | 2.6 | 318 | 61.6 | 4.17 | 141.2 |
| 7 | 90 | – | 4.33 | 473 | 24.7 | 5.26 | 151.0 |
| 8 | 90 | – | 4.79 | 617 | 13.6 | 5.91 | – voids |
| 9 | 90 | – | 3.92 | 534 | 27.7 | 4.38 | 157.5 |
| 10 | 90 | – | 3.2 | 433 | 38.2 | 3.72 | 155 |
| 11 | 70 | – | 3.12 | 409 | 17.1 | 4.61 | voids |
| 12 | 70 | – | 4.1 | 511 | 17.3 | 6.55 | voids |
| 13 | 80 | – | 3.77 | 510 | 20.4 | – | – |
| 14 | 80 | 150 | 3.64 | 513 | 16.9 | 6.6 | 229.4 |
| 15 | 80 | 150 | 4.44 | 729 | 11.0 | 7.62 | 258.7 |
| 16 | 80 | 180 | 4.44 | 743 | 11.6 | 8.0 | 265.9 |
| 17 | 90 | 180 | 4.05 | 694 | 14.6 | 6.79 | 258.5 |
| 18 | 90 | 180 | 4.33 | 715 | 12.2 | 8.0 | 266.5 |
| 20 | 75 | 180 | 4.14 | 482 | 16.5 | 7.33 | 249.4 |
| 21 | 75 | 220 | 4.38 | 499 | 11.5 | 7.69 | 267.9 |
| 22 | 102 | – | 3.45 | 512 | 58.9 | – | 125.5 |
| 23 | 102 | 180 | 4.11 | 536 | 17.4 | 6.67 | – |
| 45 | 85 | 220 | 4.17 | 605 | 12.0 | 6.91 | 271.0 |
| 49 | 87 | 200 | 4.58 | 639 | 13.0 | 6.93 | 267.2 |

**Table 2** Shrinkage, shrinkage stress and birefringence measurements on drawn yarns

| Sample number | Draw temperature | Nominal draw ratio $\lambda_a$ | Total network draw ratio $\lambda_T$ | Shrinkage $S$ | Peak shrinkage stress (MPa) | Birefringence $\times 10^{-3}$ |
|---|---|---|---|---|---|---|
| 54 | 87 | 1.26 | 1.35 | 0.27 | 2.22 | 35.8 |
| 55 | 87 | 1.30 | 1.39 | 0.34 | 2.71 | 38.3 |
| 56 | 87 | 1.66 | 1.78 | 0.43 | 4.63 | 67.9 |
| 57 | 87 | 1.86 | 1.99 | 0.51 | 5.76 | 79.3 |
| 58 | 87 | 2.14 | 2.29 | 0.55 | 7.27 | 102.5 |
| 10 | 90 | 3.2 | 3.42 | – | 17.3 | 155.0 |
| 28 | 85 | 2.9 | 3.10 | – | 12.5 | 158.0 |
| 1 | 80 | 3.1 | 3.32 | 0.65 | 22.2 | 179.2 |
| 2 | 80 | 3.24 | 3.47 | 0.55 | 21.3 | 193.8 |
| 3 | 80 | 3.77 | 4.03 | 0.36 | 16.3 | 194.5 |
| 4 | 80 | 4.32 | 4.62 | 0.12 | 39.2 | 208.7 |
| 6 | 80 | 2.6 | 2.78 | 0.63 | 9.2 | 141.2 |
| 7 | 90 | 4.33 | – | – | 64.6 | 151.0 |
| 9 | 90 | 3.92 | – | – | 40.7 | 157.5 |

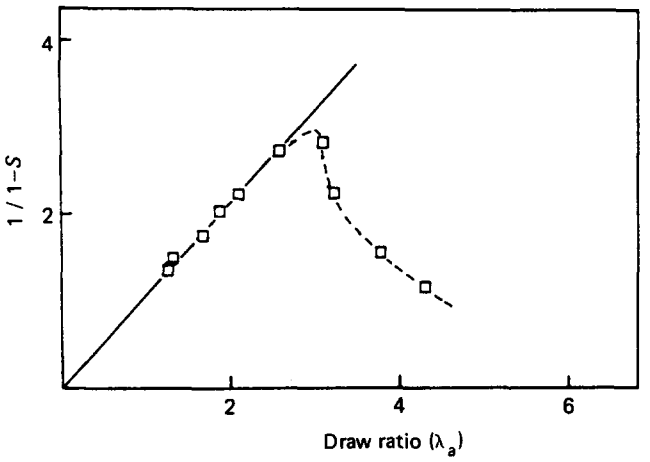


**Figure 7** Shrinkage as a function of actual draw ratio $\lambda_a$

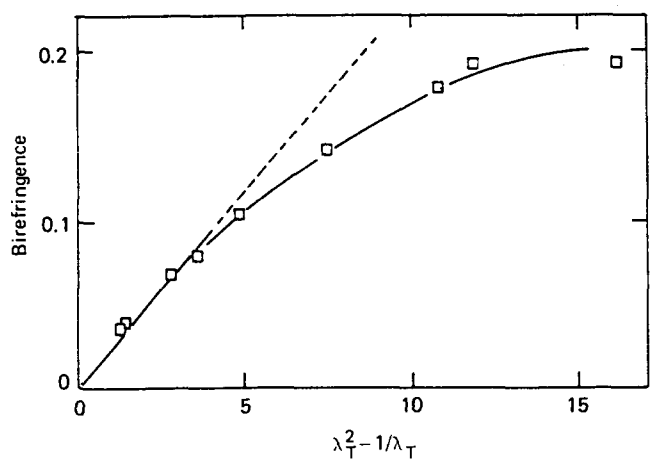


**Figure 8** Birefringence as a function of the total extension ratio $\lambda_T$

as the birefringence extension ratio relationship now passes through the origin.

*Peak shrinkage stress measurements*

From simple rubber elasticity theory the tensile drawing stress $\sigma$ is related to the total network extension ratio $\lambda_T$ by the equation:

$$\sigma = N_0 kT(\lambda_T^2 - \lambda_T^{-1}) \quad (3)$$

where $k$ is Boltzmann's constant and $T$ is the drawing temperature. Therefore, from equation (1) the stress optical coefficient $\Delta n/\sigma$ is given by:

$$\frac{\Delta n}{\sigma} = \frac{2\pi}{45kT}\left[\frac{\bar{n}^2+2}{\bar{n}}\right]^2(\alpha_1 - \alpha_2) \quad (4)$$

The frozen-in stress produced by the drawing process when the yarn is cooled below $T_g$ while under the drawing tension, manifests itself as an equivalent shrinkage stress when the sample is reheated to a temperature just above $T_g$ while being held at constant length. This shrinkage stress decays due to the chains pulling through the network entanglement points as the overall entropy of the system is increased. For PPS yarns drawn to high draw ratios this stress decay was small, gradually approaching zero as the network was drawn closer to its limiting extension and crystallization in the drawn yarn prevented any further change in the network. The shrinkage stress decay curves did not give evidence of further crystallization in any of the yarns during the measurement.

*Figure 9* shows the peak shrinkage stress plotted as a function of birefringence. It is interesting to compare these results with data published for other polymers, namely PET[4] and PEMT[7]. The stress optical coefficient for PPS drawing is a constant until quite high values of the birefringence are achieved, which suggests that the network properties remain unchanged until the draw ratio approaches a value of 2.6 and the birefringence is 0.14. In this respect PPS is similar to the amorphous polymer PEMT. In contrast PET only obeys the simple theory up to a limiting draw ratio of 1.6 and a birefringence of 0.01.

In attempting to achieve optimum mechanical properties in PPS by drawing to draw ratios greater than 3 a rapid rise in peak shrinkage stress was observed, corresponding to a steep rise in the drawing stress. This suggests that the limiting extensibility of the PPS network had been reached, and that molecular entanglements are strong enough to prevent further chain alignment. In addition stress-induced crystallization was seen to occur at this orientation which also prevented chain slippage and further increases in orientation. The shrinkage measurements show that crystallization is the primary mechanism which prevents further extension of the network, and the negligible shrinkage stress decay in the highly drawn samples further confirms that once some crystallization has occurred, this and the remaining entanglements effectively prevent further drawing from taking place.

Some shrinkage stress results are shown in *Figure 9* for yarn drawn at a higher draw temperature. The initial linear part of the curve indicates that the stress optical coefficient falls slightly at higher draw temperatures, but the results also show that the peak shrinkage stress rises steeply at lower birefringence. This result is consistent

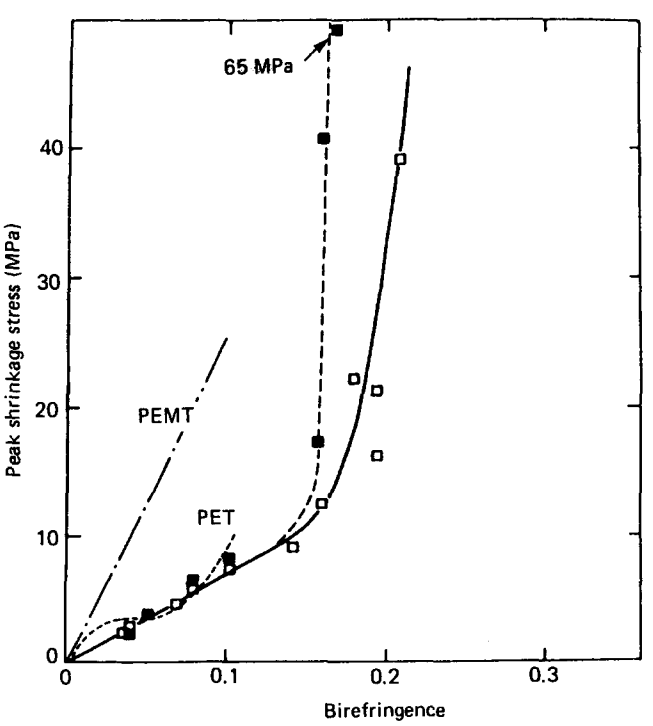


**Figure 9** Peak shrinkage stress as a function of birefringence. □, pin 85°C; ■, pin 92°C

with the description of the network for PET given by Brody[9] in which, at higher draw ratios, the network is constrained by a proportion of the chains between entanglements which constitute a 'shortest path' route in the network in the draw direction. At higher draw temperatures a lower stress is available to align chain ends and network segments not contained in this 'shortest path' network. If, at higher draw temperatures, the entanglements in the 'shortest path' network are still strong enough to determine the limiting extensibility, it is clear that this limit can now occur at a lower overall birefringence. The rise in peak shrinkage stress near the limiting extensibility is noticeably steeper for PPS than for PET. This suggests that once some crystallization has occurred the remaining entanglements in the amorphous regions of the PPS network are particularly strong.

## DERIVATION OF PPS MOLECULAR NETWORK PROPERTIES

From the shrinkage and shrinkage force measurements shown in *Figures 8* and *9* and an estimate of the polarizability of the PPS monomer unit, the molecular network parameters were calculated and compared with those for PET and PEMT in the light of their known mechanical properties.

### *Optical anisotropy of the PPS monomer unit*

Estimates for most of the bond polarizabilities are given in previous papers[11,12], but we have calculated the polarizability of the sulphur carbon bond using equations given by Denbigh[13] and a value of the bond length given by Tabor[14]. This gave the polarizability of the C–S bond along its length $b_l = 32.64 \times 10^{-25}$ cm$^3$, and the transverse bond polarizability $b_t = 18.6 \times 10^{-25}$ cm$^3$. From the crystal structure given by Tabor the optical anisotropy of the monomer unit $C_6H_4S$ along the chain axis was calculated to be $0.347 \times 10^{-29}$ m$^3$.

### *Network parameters*

From the slope of the initial linear part of the curve in *Figure 9* the stress optical coefficient for PPS drawn at 87°C was $1.31 \times 10^{-8}$ m$^2$ N$^{-1}$. The measured value of the mean refractive index of PPS fibres was 1.83 and therefore from equation (4) the polarizability of the random link was $(\alpha_1 - \alpha_2) = 2.97 \times 10^{-29}$ cm$^3$ and the average number of monomer units per random link was 8.6.

From the slope of the initial linear portion of the curve in *Figure 8* and values of the mean refractive index $\bar{n}$ and the polarizability of the random link $(\alpha_1 - \alpha_2)$ the mean value of $N_0$, the number of chain segments per unit volume was $2.87 \times 10^{26}$ m$^{-3}$. Taking the amorphous density as 1.32 g cm$^{-3}$ the average number of monomer units per chain segment was 25.85 and finally from these results the average number of random links per chain segment in the PPS network was 3.0.

### *The maximum theoretical birefringence*

From the calculated values of the polarizability of the monomer unit, the refractive index parallel and perpendicular to the chain axis can be calculated using the Lorentz–Lorenz equation:

$$n_x^2 = \frac{8/3\pi\langle P_x\rangle + 1}{1 - 4/3\pi\langle P_x\rangle}$$

where $\langle P_x\rangle$ the mean polarizability of the PPS sample per unit volume in the $x$ direction,

i.e.

$$\langle P_x\rangle = \frac{\rho N}{M} \times \frac{p_1 + p_2}{2} \qquad \text{and} \qquad \langle P_z\rangle = \frac{\rho N}{M} \times p_3$$

where $p_3$ is the polarizability of the monomer unit in the chain axis direction, $p_2$ at right angles to this direction, and $p_1$ perpendicular to both these directions.

Using the calculated values of polarizability for the C–S bond estimated above, values for the isotropic refractive index $\bar{n}$ of 1.65 and for the maximum birefringence $\Delta n_{max}$ of 0.25 are obtained. These values are both rather low compared to experimental values. The measured isotropic refractive index was 1.83 which requires a somewhat higher value for the polarizability of the C–S bond, i.e. $47 \times 10^{-25}$ cm$^3$ compared with the value $b_l = 32.6 \times 10^{-25}$ cm$^3$ calculated previously. This does not look unreasonable since the value given by Denbigh[12] for the polarizability of the C=S bond is $75.5 \times 10^{-25}$ cm$^3$.

Using the higher value of $47 \times 10^{-25}$ cm$^3$ for the polarizability of the C–S bond the optical anisotropy of the monomer is calculated as $0.41 \times 10^{-23}$ cm$^3$ and the corresponding value for the maximum birefringence is 0.333. Assuming the higher value of polarizability for the C–S bond also slightly alters the calculated network parameters, giving 7.3 monomers per random link and 3.6 random links per chain segment.

The higher value of 3.6 random links per chain is more likely to be correct in view of the linear region of the birefringence draw ratio relationship in *Figure 8*, but statistically this is still an unrealistically low value.

## DISCUSSION

The mechanical properties achieved in low speed pin and plate drawing of PPS yarns are rather lower than those for PET drawn to similar high draw ratios, but they are similar to the properties of PEMT. In particular, the initial modulus of PPS is 8 GPa which compares with 16 GPa obtained with PET. The failure stress of PPS fibres is at best 740 MPa compared with 1.1 GPa obtained with PET. However the degree of molecular orientation achieved in highly drawn PPS and PET fibres is similar, being in both cases just greater than 80% of the theoretical birefringence of fully aligned chains. The lower modulus of PPS fibres compared with PET therefore does not seem to be due to a failure to achieve a high enough molecular orientation in the drawing process, although there may be small differences in the orientation of the amorphous regions of the fibre, which have not been determined in this investigation but which might contribute in part.

However of greater significance are recent determinations of the experimental crystal modulus and theoretical chain modulus of PPS[2] which have shown that the crystal modulus of PPS has a value in the range 40 GPa which is approximately half the crystal modulus of PET. Since the largest contribution to the crystal compliance of PPS derives from opening of the C–S–C bond angle, the zig-zag molecular conformation suggested by Tabor for the crystal structure, would, if present in the oriented amorphous chains, be largely responsible for the lower modulus of drawn PPS fibres. A

**Table 3** Network parameters for PPS, PET and PEMT

| Network parameters | PPS | PPS | PET | PEMT |
|---|---|---|---|---|
| Drawing temperature (°C) | 87 | 87 | – | 70 |
| Shrinkage temperature (°C) | 100 | 100 | 70 | 70 |
| Stress optical coefficient $\Delta n/\sigma \times 10^{-9}\,N^{-1}\,m^2$ | 13.1 | 13.1 | 5.5 | 3.56 |
| Optical anisotropy of the random link ($\times 10^{-23}\,cm^3$) | 2.97 | 2.97 | 1.51 | 0.94 |
| No. of monomers per random link | 8.6 | 7.3 | 2.9 | 2.3 |
| No. of chain segments per unit volume ($\times 10^{26}\,m^{-3}$) | 2.87 | 2.87 | 1.89 | 2.15 |
| No. of monomers per chain segment | 26 | 26 | 23.4 | 18 |
| Optical anisotropy of monomer unit ($\times 10^{-23}\,cm^3$) | 0.347 | 0.407 | 0.52 | 0.408 |
| No. of random links per chain segment | 3.0 | 3.6 | 8.0 | 8.0 |
| Polarizability of C–S bond $b_1$ ($\times 10^{-25}\,cm^3$) | 32.64 | 47.0 | – | – |

similar zig-zag conformation has been proposed for the conformation of the amorphous polymer PEMT[7] to explain low modulus results compared to PET.

Comparison between the network parameters of PPS, PET and PEMT in *Table 3* shows that the PPS network contains significantly more chain segments per unit volume and therefore has a higher density of entanglement points with stiffer chains between them than either PET or PEMT. The chain segments between entanglements contain similar numbers of monomer units in each of the three polymers, but the PPS monomer unit is smaller without the several flexible links in the PET and PEMT molecules. In addition the high electron density of the sulphur and phenylene groups may restrict free rotation of the C–S bond. These molecular considerations support the view derived from shrinkage and shrinkage force measurements analysed on the basis of the simple rubber elasticity model, namely that the PPS network is more tangled and constrained than either the PET or PEMT networks.

From consideration of the peak shrinkage stress results in *Figure 9* there is no evidence that the PPS network is modified by the drawing process, in contrast to PET where some breakdown of entanglement points has been proposed to explain the plateau in the shrinkage stress measurements. *Figure 9* confirms that crystallization in PPS drawn at 85°C is delayed until quite high birefringences are achieved and the network is close to its limiting extension. The plateau in the shrinkage stress curve for PET is known to be drawing temperature dependent, as is the slope of the curve for PEMT. However, although only a limited range of draw temperatures have been investigated for PPS the present results suggest that the mechanical properties of PPS are unlikely to be greatly improved by changes in drawing conditions. The inclusion of an annealing and hot stretching zone in the drawing process results in only small improvements in the initial modulus and failure stress of PPS yarns, although there is a more significant increase in birefringence.

## CONCLUSIONS

PPS multifilament yarn can be drawn over a heated pin to high values of molecular orientation and for these yarns the ratio $\Delta n/\Delta n_{max}$ is similar to that of highly drawn PET yarns. The increase in orientation of PPS yarns with draw ratio also approximates to the simple rubber elasticity model until quite high values of draw ratio and birefringence. However, comparison of the network parameters of PPS and PET suggest that the PPS network is rather more constrained with a higher density of entanglements with fewer, more rigid links between them. This appears to delay the onset of stress induced crystallization, but when crystallization does occur a further small increase in draw ratio causes a steep rise in drawing stress showing that the network reaches its limiting extensibility quite rapidly at this point.

The highest initial modulus of PPS yarns was 8 GPa compared with 16 GPa achieved with PET yarns drawn to a similar extensibility. This is attributed to the planar zig-zag conformation proposed for the molecule in the crystal phase and the C–S–C bond angle of 110°, rather than failure to achieve a sufficiently high orientation.

Although a limited range of drawing and annealing temperatures have been studied the considerations above suggest that the mechanical properties of PPS filaments, determined by this investigation, are unlikely to be greatly exceeded.

## ACKNOWLEDGEMENTS

The authors wish to thank Phillips Petroleum Company who supported this work and colleagues in the Physics Department at Leeds University for helpful discussions.

## REFERENCES

1 Ito, M. and Porter, R. S. *J. Polym. Sci.* 1985, **23**, 245
2 Unwin, A. P. and Ward, I. M., to be published
3 Pinnock, P. R. and Ward, I. M. *Br. J. Appl. Phys.* 1964, **15**, 1559
4 Rietsch, F., Duckett, R. A. and Ward, I. M. *Polymer* 1979, **20**, 1133
5 Faust, R. C. and Marrinan, H. J. *Br. J. Appl. Phys.* 1956, **6**, 351
6 Capaccio, G. and Ward, I. M. *Colloid Polym. Sci.* 1982, **260**, 46
7 O'Neill, M. A. *Ph.D. Thesis*, Leeds University (1985)
8 Padibjo, S. R. and Ward, I. M. *Polymer* 1983, **24**, 1103
9 Brody, H. J. *Macromol Sci. Phys.* 1983, **B22**(3), 407
10 Kuhn, W. and Grün, F. *Kolloid-Z.* 1942, **101**, 248
11 Bunn, C. W. and Daubeny, R. de P. *Trans. Faraday Soc.* 1954, **50**, 1173
12 Pinnock, P. R. and Ward, I. M. *Trans. Faraday Soc.* 1966, **62**, 1308
13 Denbigh, K. G. *Trans. Faraday Soc.* 1940, **36**, 936
14 Tabor, B. J., Magré, E. P. and Boon, J. *Eur. Polym. J.* 1971, **7**, 1127
15 Kashiwagi, M., Cunningham, A., Manuel, A. J. and Ward, I. M. *Polymer* 1973, **14**, 111

### Note added in proof

Recent work has thrown doubt on the validity of this suggestion for the conformation of PEMT. The value of the optical anisotropy of the monomer unit given in *Table 3* may therefore be too low by a maximum of 20% with a corresponding increase in the number of random links per chain segment.